SEVENTH EUROPEAN ROTORCRAFT AND POWERED LIFT AIRCRAFT FORUM

Paper No. 43

HELICOPTER ROTOR DOWNWASH RESULTS OF EXPERIMENTAL RESEARCH AT THE DFVLR-ROTOR TEST STAND AND THEIR COMPARISON WITH THEORETICAL RESULTS

B. Junker, H.-J. Langer

Deutsche Forschungs- und Versuchsanstalt für Luft- und Raumfahrt e.V., Institut für Flugmechanik
Braunschweig, Germany

September 8-11, 1981

Garmisch-Partenkirchen
Federal Republic of Germany

Deutsche Gesellschaft für Luft- und Raumfahrt e.V.
Goethestr. 10, D-5000 Köln 51, F.R.G.

HELICOPTER ROTOR DOWNWASH
RESULTS OF EXPERIMENTAL RESEARCH AT THE DFVLR-ROTOR TEST STAND AND THEIR COMPARISON WITH THEORETICAL RESULTS

B. Junker, H.-J. Langer

Deutsche Forschungs- und Versuchsanstalt für Luft- und Raumfahrt e.V., Institut für Flugmechanik
Braunschweig, Germany

ABSTRACT

In recent years the system tests and dynamic researches at the rotor test stand were compared with several downwash measurements. It was the objective of these experiments to obtain reliable results to investigate the validity of the downwash calculations. It is necessary mainly to demonstrate the dependency between mathematical parameter values and rotor control values e.g. thrust, advance ratio and control angles.

For comparisons mathematical models like the local momentum theory, and a fixed vortex model - both are very rapid in calculation of downwash - were applied.

For these experiments a four-bladed hingeless rotor and a two-bladed See-Saw rotor with an advance ratio of up to $\mu = 0.2$ were used. Numerous tests were realized to study the flow field of rotor downwash in different windtunnels. The windtunnel of the Volkswagenwerk in Wolfsburg was the first one, then the Daimler-Benz windtunnel at Stuttgart. Both have a semi-open test section. Lastly the new, closed 8 x 6 m test-section from the DNW.

The measuring equipment for the downwash was set up on both sides of the rotor stand. So it was possible to receive two values at the same time. The measuring range was restricted to the rotor positions $\psi = 90^{\circ}$ and $\psi = 270^{\circ}$ (x/R=0) over the whole rotor diameter up to 14 defined points. The probe position to the rotor plane was varied between $z/R = 0.02$ and $z/R = 0.3$.

For the measurements two probe systems were used. At first pneumatic probes were applied, that gave acceptable mean values, and then hot-wire probes in X-configuration were used to investigate downwash dynamics in more detail. Measurements were conducted in the x-z-plane. Windtunnel test results, correlation aspects to the mathematical models and errors will be discussed.

PARAMETER LIST

(4-bladed Hingeless Rotor)

rotor diameter [m]	4
blade chord, constant [m]	0.121
twist, linear [^{o}/m]	-4
blade profile	NACA 23012 mod.
profile beginning, [m] from shaft axis	0.44
preconing [^{o}]	∅
rotor frequency [Hz]	≈17.5
depending on atmospheric condition	
blade tip speed [m/s]	220
solidity [-]	0.077
center of gravity of [-] profile	0.23
spring constant, flapping [Nm/^{o}]	-7.266
equivalent flapping hinge offset [m]	0.27
blade mass [kg] of flapping blade	1.41
Mass moment round flapping hinge [kgm]	1.195
Moment of inertia with respect to the flapping hinge [kgm^{2}]	1.358
Ma-number	0.645
Re-number/Ma-number	$1.97 \cdot 10^{6}$
Froude-number	49.2
Lock-number (INA, 0 m)	4.54

PARAMETER LIST
(2-bladed See-Saw Rotor)

rotor diameter [m]	4
blade chord, const. [m]	0.19
twist, linear [^{o}/m]	-5
blade profile	NACA 63_3 - 018
profile beginning [m]	0.8
preconing [^{o}]	$0^{o}54'$
rotor frequency [Hz], depending on atmospheric condition	≈17.5
blade tip speed [m/s]	220
solidity [-]	0.061
blade mass [kg]	8.390
Ma-number	0.642
Lock number (INA, Ø m)	5.095

INTRODUCTION

Results will be presented from downwash measurements under two different rotors

- a four-bladed hingeless rotor
- a two-bladed tethering rotor

The measurements were conducted in three different windtunnels with highly different test-section shapes: closed and semi-open, rectangular and semi-open/semi-oval.

The downwash velocities were measured by two different sensors

- a 5-hole pressure probe measuring three components of the downwash
- a hot-wire anemometer measuring two components of the downwash

The probes were installed under both sides of the rotor, the side at the advancing blades ($\psi = 90^{o}$) and at the side of the retreating blades $\psi = 270^{o}$. Due to the flapping motion of the rotor blade the distance between blade section and probe varies slightly.

Emphasis was placed on the rotor behavior at low forward speeds; therefore most of the measurements were conducted at advance ratios of $\mu = 0.04$, $\mu = 0.05$, and $\mu = 0.1$.

In order to develop an advanced and fast computer program for downwash calculation to be used for a helicopter simulation program and in order to evaluate the efficiency of this program, two different relatively simple mathematical models were tested and compared with measured data:

- a modified local momentum theory
- a rigid wake theory

Both theories are presented briefly. Comparing measured and calculated data benefits and disadvantages of the programs are discussed in detail.

MEASURING EQUIPMENT

The facility to measure the downwash was installed on both sides of the test stand (fig. 1 and fig. 2). The facility can be tilted simultaneously with the rotor plane. So measurements are referred to body fixed coordinates. In lateral direction the measured region includes the whole rotor diameter. The distance between sensor and rotor plane is adjustable. Measurements were realized at distances between $z/R \approx 0.02$ m and $z/R = 0.3$ m at $x/R = 0$. Variation in x-direction is not possible up to now. As the z/R positioning is fixed during a test serie , the sensor can be moved electrically on both sides of the rotor in y/R direction. Due to the simplification of calibration the sensors are adjustable to the main flow direction in the x-z plane. Conrad vector probes [7] are mainly applied (fig. 3). Pressure signals are indicated on alcohol filled U-shaped manometers. The difference in the level of liquid indicates the pressure.

A two-element, hot-wire anemometer was placed for the acquisition of instationary flow (fig. 4). This probe can measure the flow in the x-z plane. The two signals are referred to the blade position. Flow components out of x-z plane may cause an error. The X-probe anemometer was developed by the DFVLR [8].

DATA ACQUISITION AND EVALUATION

Data Acquisition of the 5-hole pressure probe was realized by a photo camera.Amongst the pressure level of the U-monometers, position and angle of incidence of the probe in the x-z plane were shot by a camera. The measurement started when the indicated pressure of the angle position of the probe is compensated. The measuring procedure of 14 radial positions lasts three minutes.

A special facility transmits the velocity data from the photos to punched cards. Via a Fortran program the velocity data are split in the three body fixed axis.

The signals of the X-hot-wire probe were recorded on tape via PCM-telemetry (16 channels, 125 kbit/s, 10 bit resolution). Recording a serie of 14 data points requires about 10 minutes, due to tape recording of the data.

Recording the measured values, the data are digitized and a FFT (Fast Fourier Transform) was executed. Due to the limited bit rate of the telemetry, data higher than 9^{th} order are suppressed. The results are correlated with calibrated data to generate the flow velocities (WX, WZ) and flow angle (ALF). The calibration matrix was realized in a small test tunnel by variation of speed, flow angle and temperature. Results of a test run in the DNW-windtunnel are presented in fig. 6.

WINDTUNNEL MEASURING PROGRAM

The downwash components (w_x - positive forward, w_y - positive to the right, w_z - positive downward) were determined as a function of thrust, advance ratio, rotor angle of attack, radial and vertical position.

The region of variation of these parameters were:

$$0.15 \leq r/R \leq 1.05$$
$$0.02 \leq z/R \leq 0.3$$
$$1000\ N \leq P_z \leq 5000\ N$$
$$0 \leq \mu \leq 0.2$$
$$-10^{o} \leq \alpha_{Ro} \leq +7^{o}$$

Only one test run was necessary for the parameter variation of r/R. Fig. 5 shows the measured stream vectors in the vicinity of the rotor.

Hot-wire measurements are combined with pressure probe measurements. At $z/R = 0.3$ a pressure probe, at $z/R \approx 0.02$ the hot-wire probe was positioned.

Fig. 2 shows the downwash rig with the pressure probes on both sides of the rotor test stand. On the left side the hot-wire sensor is positioned very near to the rotor.

LOCAL MOMENTUM THEORY

The mathematical model of a rotor is based on the concept to represent an actual aerodynamic load and downwash distribution of a blade by a series of n overlapping elliptical wings with decreasing size; each of these wings has an elliptical circulation along the span and therefore produces an uniform downwash velocity. Each elliptical wing is arranged to be onesidely drawn to the blade tip. By neglecting the upwash flow outside the wings, which have an elliptical circulation distribution, the induced velocities of the blade is given by the sum of the constant induced velocities of each elliptical element [2].

The theory considers

- the upwash flow outside the rotor blade when the rotor is advancing
- the vortex interaction between the preceeding blades tip vortex and the following blade
- the attenuation of the circulation of the advancing blade when it is hitting the succeeding blade
- blade flapping motion .

The theory does not consider

- vortex/vortex interaction
- flow separation due to instationary effects
- any distortion of the rotor wake
- the wake contraction and roll up.

Some empirically determined parameters were used in the calculations in order to base the calculation on rotor measurements as well as to reduce the computation time. Three influence factors are important

IF(1) - Factor considering the interaction between preceding and following blade

IF(2) - Attenuation of tip vortex

IF(3) - Correcting parameter. It decreases with the advance ratio and determines the rotor downwash so that measured and calculated thrust are in agreement.

Based on various hot-wire anemometer measurements, IF(1) was defined to be constant at 0.85. IF(2) highly depends on the number of chosen segments along the blade radius.

As a tip loss factor is not taken into account and the upwash outside the blade influences the induced velocities at the blade tip, the IF(2) - influence factor has to be fitted appropriately. The factor IF(3) takes globally into account the downwash field according to a preselected thrust. This factor is comparable with the coefficient C in [2].

Comparisons of the calculated and measured data show that the best agreement was obtained when a constant blade chord for each elliptical blade element was assumed in the calculation for hovering condition and low advance ratios.

Furthermore, theoretical data are more reliable when the calculations take into account the flapping coefficients. The influence of flapping shows figure 7 for a trimmed flight with $\alpha_{Ro} = 0^{o}$. The flapping coefficients are derived from measured blade flapping moment data. Especially the determination of the flap angle is not very accurate due to the characteristics of a hingeless rotor: the flapping hinge is not clearly defined, higher orders of flapping modes, and a strong coupling between flapping and lagging due to blade pitch angle changes. As the flapping moment is proportional to the flap stiffness in the first iteration, both, flap angle magnitude and phase are calculated by dividing the blade root flapping moment by the spring stiffness factor. In contrast to hingeless rotors the flapping angle measurement for the two-bladed tethering rotor is relatively simple. A sensor at the central hinge and another one at the blade pitch link are necessary to obtain the input data for the local momentum calculation.

Nevertheless, calculated and measured data points may vary considerably in spite of well known coefficients. Wind tunnel flow at low advance ratios and small rotor angle of attack may cause a highly distorted flow through the rotor disk so that calculation yields no reliable data.

When a downwash calculation is taken to evaluate rotor forces and moments in the body-axis system, results can be completely wrong because of the sensitivity of the phase to rotor components.

The computer program needs a CPU-time of 6 sec (Siemens 7.870) and a memory of 80 kbyte.

The program needs following input data:

- geometry sizes of the rotor
- profile-data
- windtunnel speed
- rotor angle of attack
- descent-or climb velocity
- blade twist
- rotor frequency
- thrust
- control angles
- flapping coefficients.

RIGID WAKE ANALYSIS

As the analysis is supposed to be well-known, it is important to know how the input data are generated. The computer program needs as input data the

- flapping distribution $\beta = f(\psi)$
- normal and tangent velocities $v_N = f(r, \psi)$, $v_T = f(r, \psi)$
- local lift distribution $l = f(r, \psi)$

The hingeless rotor blade is assumed to be rigid, with an equivalent flapping hinge and equivalent spring stiffness.

Solving the differential equation for the flapping acceleration [5].

$$\ddot{\beta} = \frac{1}{I_b} \left[-M_g \cos\beta - \Omega^2 (I_b \cos\beta \sin\beta + \frac{M_g}{g} e \sin\beta) - k_\beta \beta + M_\beta\right]$$

The input data for the 'Rigid Wake' program are known. The parameters in the above equation are:

I_b - flap inertia [kgm^2]

M_g - blade gravity moment [kgm]

e - equivalent hinge offset [m]

k_β - equivalent spring stiffness (flapping) [Nm/rad]

M_β - flap moment due to aerodynamic forces [Nm]

The start parameters are corrected to reach a steady state. As the blade system is heavily damped by aerodynamic forces, one rotor revolution is sufficient usually to reach a steady state. Aerodynamic forces and moments are calculated applying the local momentum theory considering also calculated flapping angles. The computer program needs 50 seconds to solve the differential equation, the required memory is 81 kbyte. In contrast to the local momentum theory the rigid wake computer program calculates the rotor induced velocities at each point of the flow field. This is important when measured and calculated data are compared, because of the distance between blade and sensor.
The computation time of the rigid wake program depends on several pre-selectable settings:

The number of rotor revolutions, the number of vortices, the contraction, the roll-up of the flow field, and the iterative calculation of the core size diameter which depends on the rotor loading.

The computation time of the rigid wake program is 200 seconds and the memory is 120 kbyte. When the program is used within a helicopter real time simulation program the computation time seems to be too long. Therefore various simplifications should be made. As we will see in the next chapter, some simplifications are possible.

RESULTS

Results will be discussed that were obtained from downwash measurements and calculations of the four-bladed rotor at

- $\mu = 0$; variable z/R (figure 8)
- $\mu = 0.1$; variable z/R (figure 9)
- $\mu = 0.04$; variable thrust (figure 10)
- z/R = const; variable μ (figure 11).

All measurements were made by a 5-hole pressure probe.

For the two-bladed rotor measurements were made at

- $\mu = 0.11$; variable z/R (figure 12 and figure 13)

by a hot-wire sensor near the blades and by a pressure probe at z/R = 0.3.

Figure 8 shows the 3-component downwash measurements at a constant thrust and at an advance ratio equal to zero. Signals measured in two different distances from the rotor are plotted. In longitudinal direction (x-direction) there is no change in velocity when the distance increases. As expected the spin of the downwash is clockwise due to the rotation of the blade. However there are significant changes in lateral direction (y-direction). Because of the pressure characteristic at the blade tip and the blade root a strong vortex should be measured. But due to the distance of the sensor from the blade the mean values of the probe do not show these effects; but contraction can clearly be seen (see also the velocity components in figure 5). At the distance of 0.6 m from the rotor plane effects from stream contraction are very small.

In the vertical direction (positive downward) the contraction effect is small so that the tip loss is only slightly drawn the rotor center.

Calculations show that the momentum theory yields relatively good agreement with measured data because two stream effects influence each other: on the one hand, due to contraction, the velocity of the downwash decreases when the distance from the rotor plane increases. This effect is considered by the rigid wake analysis but not by the local momentum theory which calculates the downwash only in the rotor plane. On the other hand the rotor operates in ground effect which causes a decrease in induced velocities under the rotor. Neither the wake analysis program nor the local momentum theory consider this fact. Therefore, in this case, local momentum theory produces better results.

In figure 9 the same parameter (z/R) is varied but the advance ratio is now $\mu = 0.1$. The local velocities in x-direction are more influenced by the downwash than by the windtunnel velocity. Due to the flow interpretation of Glauert's formula w_x should be equal to v_∞ but because of the small α_{Ro} (indicated $\alpha_{Ro} = {}^x\text{-}1^o$) the flow character through the rotor disk may be considerably different from theory. w_y shows evidently the roll up tendency of the flow similar to the fixed wing flow. At $z/R = 0.07$ the advancing blade at the root has the same contraction effects as at $\mu = 0$ and at a distance of $z/R = 0.15$ the lateral velocity at the blade root is near zero.

Measurements of w_z are influenced by the geometric character of the downwash skew: the larger the distance between rotor plane and plane of sensors the more velocities are measured from the front area of the rotor. This fact results in lower induced velocities (according to momentum theory, forward flight [1]). Measured and calculated values show no good agreement. This is caused by the small incidence of α_{Ro}. Calculated or evaluated flap angles may vary from real conditions, so that calculation can yield large errors.

Results from local momentum theory show that a wrong evaluated phase of the flap angles results in a non-trimmed flight condition. As the local momentum theory calculates induced velocities only in the rotor plane small differences between calculated and measured data are usual.

Vortex theory calculation, too, shows no good coincidence with measured data as the flapping velocities derived from equation (1) do not take into account the real aerodynamic and dynamic forces acting on an elastic rotor blade at low advance ratios and small α_{Ro}.

This interpretation will be confirmed comparing calculation and measured data in figure 10. Additionally due to the low advance ratio a ground effect exists, whose effect to the induced velocities was discussed in figure 8.

Figure 10 shows the dependence of thrust from downwash. As expected an increasing thrust produces a higher downwash. At high thrust larger variations of induced velocities occur in lateral and longitudinal direction due to $\alpha_{Ro} = 0$ and the low advance ratio. Distortion, contraction and roll up of the flow can be seen at the blade tip in lateral direction. This is caused by a high velocity gradient.

The local momentum theory doesn't consider appropriately the inner area of the rotor induced velocity field. This is because measurements were conducted below the rotor, whereas the calculation refers to the rotor plane. That means: Smoothing of the vortex field, which occurs with increasing distance from rotor plane, is not considered. The higher thrust condition could not be calculated because of a failure of the flapping moment sensor.

The vortex calculation does not consider the center of circulation at the blade as starting point of the rolled up vortex [4]. Therefore it can occur that the calculation results in a stronger flow contraction than in reality.

In figure 11 the advance ratio was varied from μ=0.05 to μ = 0.14. The thrust was nearly unchanged. Due to an $\alpha_{Ro} = -5^{o}$ the simplification of equation (1) (to consider first order flapping only) seems to be more realistic than for calculation at $\alpha_{Ro} = 0^{o}$.

At μ = 0.15 the data points in lateral direction show the influence of a fuselage, mounted for some test runs. Because of uncertainties in downwash geometry, it is sometimes too hard to explain the reasons of local flow changes of the velocity field. When the advance ratio increases the rotor produces a flow field like a fixed wing, as can be seen from the induced velocities in lateral direction. As expected the flow field in vertical direction decreases. The shape of the velocity distribution is a result of the downwash skew.

All data calculated with the vortex theory in fig. 11 are computed without roll up of the flow shed behind the rotating blade. Measured and calculated values coincide better without roll up calculation. That means: When a clean flow through the rotor ($\alpha_{Ro} = -5^{o}$) exists calculations without rolling up produce better results. Rolling up of the flow field means that after a quarter of a rotor revolution the whole vorticity of the blade is produced by a strong vortex near the blade tip.

The vortex theory as well as the local momentum theory do not consider the velocities in the vicinity of rotor axis accurately. The reason is that the local momentum theory only calculates the downwash where the blade is profiled. Therefore at the blade root the induced velocities are zero. The wake theory assumes a vortex at the blade root (when calculated without rolling up). This produces an upwash, resulting in a steep decrease of induced velocities. This may cause differences between calculated and measured values.

The downwash of the two-bladed rotor was measured in a distance of z/R = 0.3 with a 5-hole pressure probe and a X-hot-wire probe, installed as near as possible to the blade. Mean values of the hot-wire anemometer and the 5-hole probe are presented in figure 12.

It can be seen that the velocity vector of the pressure probe in x-direction is virtually identically to the windtunnel speed. Obviously the sensor is out of downwash because of its distance to the rotor plane. Measured values from the hot-wire anemometer are only reliable at r/R = 1.05 and r/R = 1.0, because a two component measurement in x- and z-direction yields a significant error, when a high lateral velocity exists.

The w_z-component shows the variation of downwash when the distance from the rotor plane increases. The mean values of the hot wire anemometer agree satisfactoryly with the calculation of local momentum theory in particular when previously discussed inaccuracies are considered.

A time history of the induced velocities of the hot-wire anemometer at an azimuth angle of 270° is presented in figures 6 and 13. In addition to the velocity components in x- and z-direction the local flow angle, the voltage signals of the two hot-wires and the effective velocity are plotted.

The analogue signals of the x-probe were digitized. Because of the limited bit rate (125 kbit/s, 16 channels, 10 bit resolution) only rotor harmonics up to the 9th order are considered. Downwash was measured at fourteen radial positions under the blade. Upwash exists outside the blade and the signal's dynamic is small. As expected, at the blade tip the dynamic component within the signal has the highest values due to the blade tip vortex.

It can be assumed that the signals have a phase error. Most of the w_z-curves show a peak at a rotor phase angle of $\psi = 90°$ whereas normally a phase lag exists between blade passing and peak of velocity [6]. At r/R = 0.89 and r/R = 0.86 a significant decrease in the peak velocity can be seen. Probably this effect results from the blade tip vortex of the preceding blade. The mid-blade region has a smooth flow field. Due to the blade root vortex, the dynamic values increase at the blade root.

CONCLUDING REMARKS

In this study results of two different downwash computer programs are compared with measured data. The shortcomings of this correlations were:

1. The local momentum theory considers local velocities in the rotor plane. Measurements are made in different distances below the rotor. So inaccuracies between measured and computed data are possible.

2. The rigid vortex theory and the local momentum theory require the flapping coefficients as input data. Inaccuracies of these coefficients can produce differences between calculated and measured velocities.

3. Evaluation of flapping angles from measured blade bending moments can cause errors especially at high advance ratios where strong coupling among flapping, lagging and torsion occur.

4. The measurements are influenced by ground effect at low advance ratios and at low α_{Ro}.

With respect to the objectives of this study the following conclusions can be drawn:

- The two component hot-wire measurement system is considered to produce accurate data, when the third component is small. The 5-hole pressure probe is a very simple and useful system to measure mean values with high accuracy.

- At small α_{Ro}-angle, the vortex computer program yields better results when the calculation considers a rolled up flow behind the rotor blade.

- The local momentum theory is a valuable program to calculate input data for the wake analysis program.

The goal of this correlation study was to develop, to improve and to verify a mathematical downwash representation which is suitable for simulation models in the field of flightmechanics. Encouraging results could be reached in some areas, but there are still some shortcoming in theoretical as well as in experimental items.

Future efforts will concentrated on further improvement of windtunnel test techniques and on adaptation of the downwash models to extensive simulation programs.

REFERENCES

[1] Johnson, W.: Helicopter Theory, Princeton University Press, 1980

[2] Stepniewski, W.Z.: Rotary Wing Aerodynamics, Vol. 1, Nasa Contractor Report 3082, 1979

[3] Junker, B.: Zusammenfassung der Abwindmessungen am Rotorversuchsstand, DFVLR IB 154-78/30, 1978

[4] Bergmann,H. Fuhr, J.W.: Parameteruntersuchungen zur Rotorabwindberechnung. Einfluß auf die Umströmung eines Flügels. DLR FB 70-62, 1970

[5] Lehmann, G.: Ermittlung des optimalen periodischen Verlaufs des Einstellwinkels eines Hubschrauber-Rotorblattes, DFVLR, IB 154-78/2, 1978.

[6] Caradonna, F.X., Thung, C.: Experimental and Analytical Studies of a Model Helicopter Rotor in Hover. Paper No. 25, 6th European Rotorcraft and Powered Lift Aircraft Forum Bristol, 1980.

[7] Conrad, O.: Geräte zur Messung von Strömungsrichtungen, ATM-Blatt V, 116-2, 1950.

[8] Froebel, E.: Beschreibung und Betriebsanleitung zum Hitzdrahtanemometer HDA III, DFVLR IB 357-76/11, 1976.

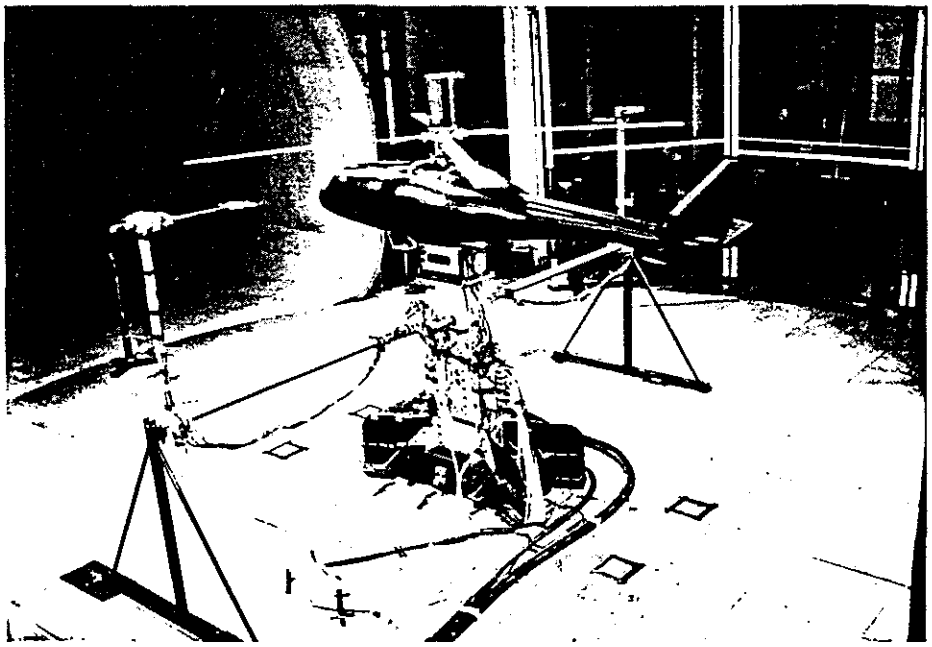

Fig. 1 Rotor Test Stand in the Daimler-Benz Windtunnel (open test section)

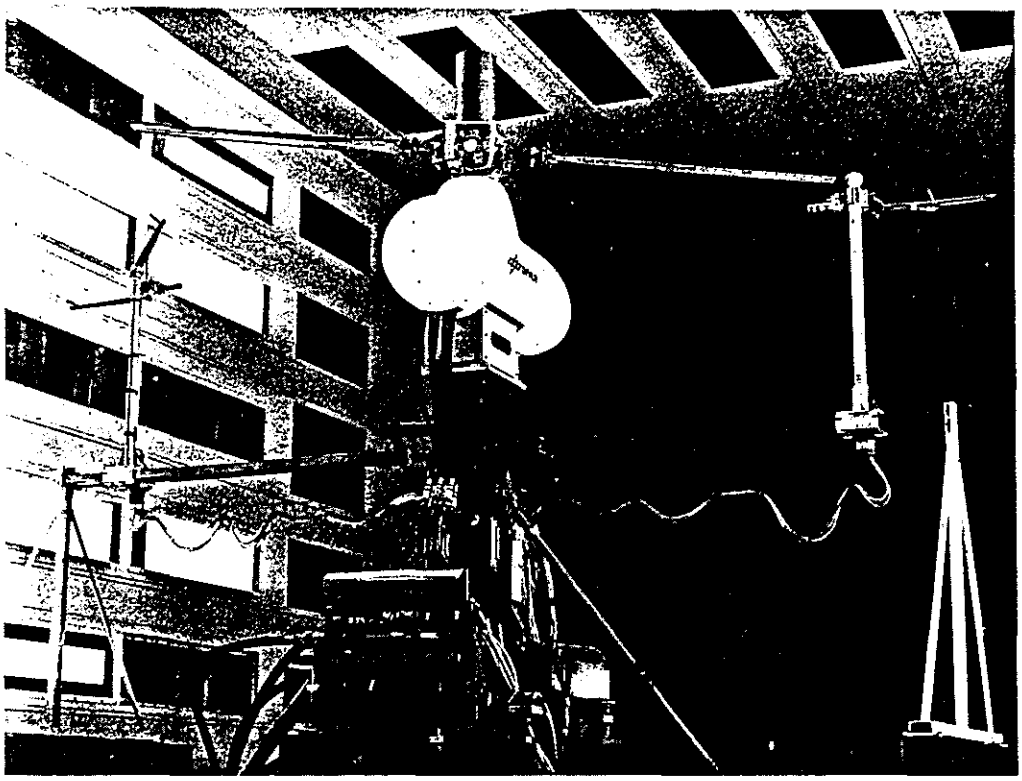

Fig. 2 Rotor Test Stand in the German-Dutch Windtunnel (closed test section)

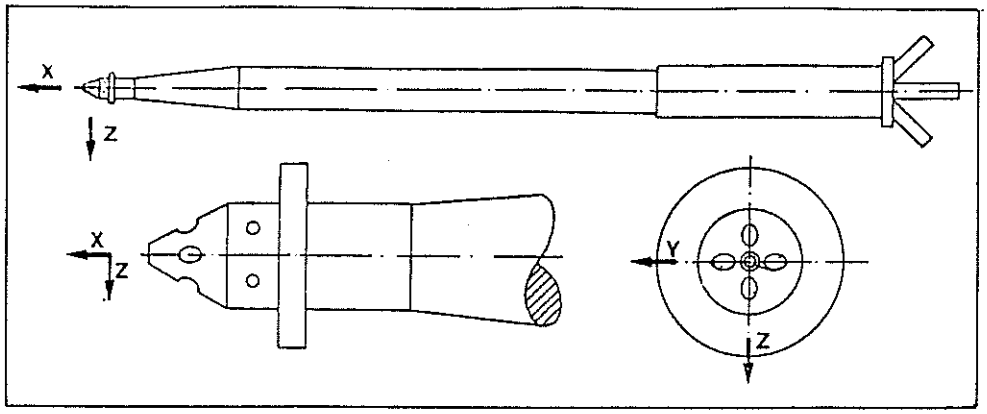

Fig. 3 Pneumatic vector probe (by Conrad)

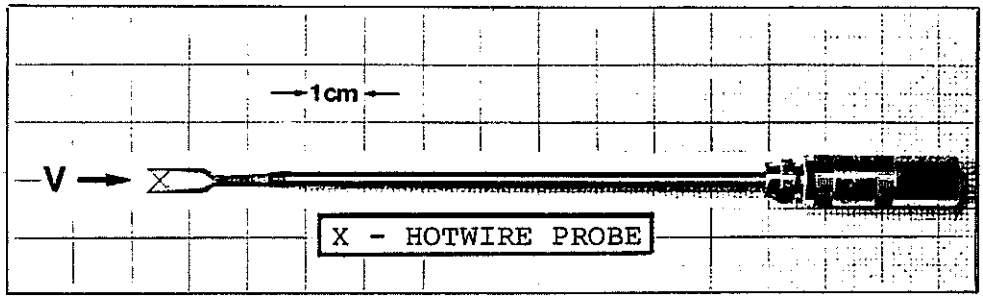

Fig. 4 Hot-wire anemometer

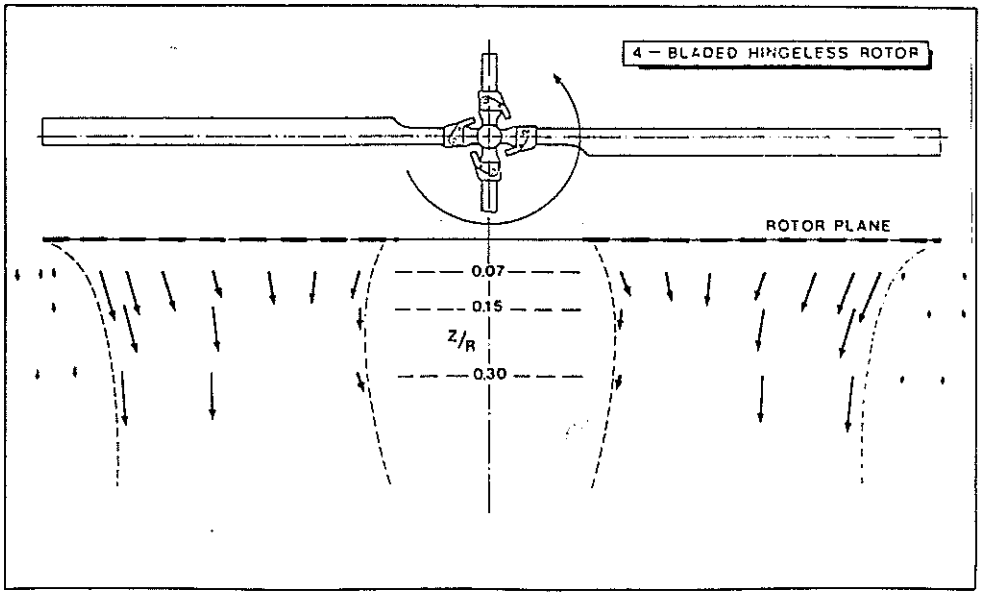

Fig. 5 Velocity vectors in the Y-Z plane in hover (IGE)

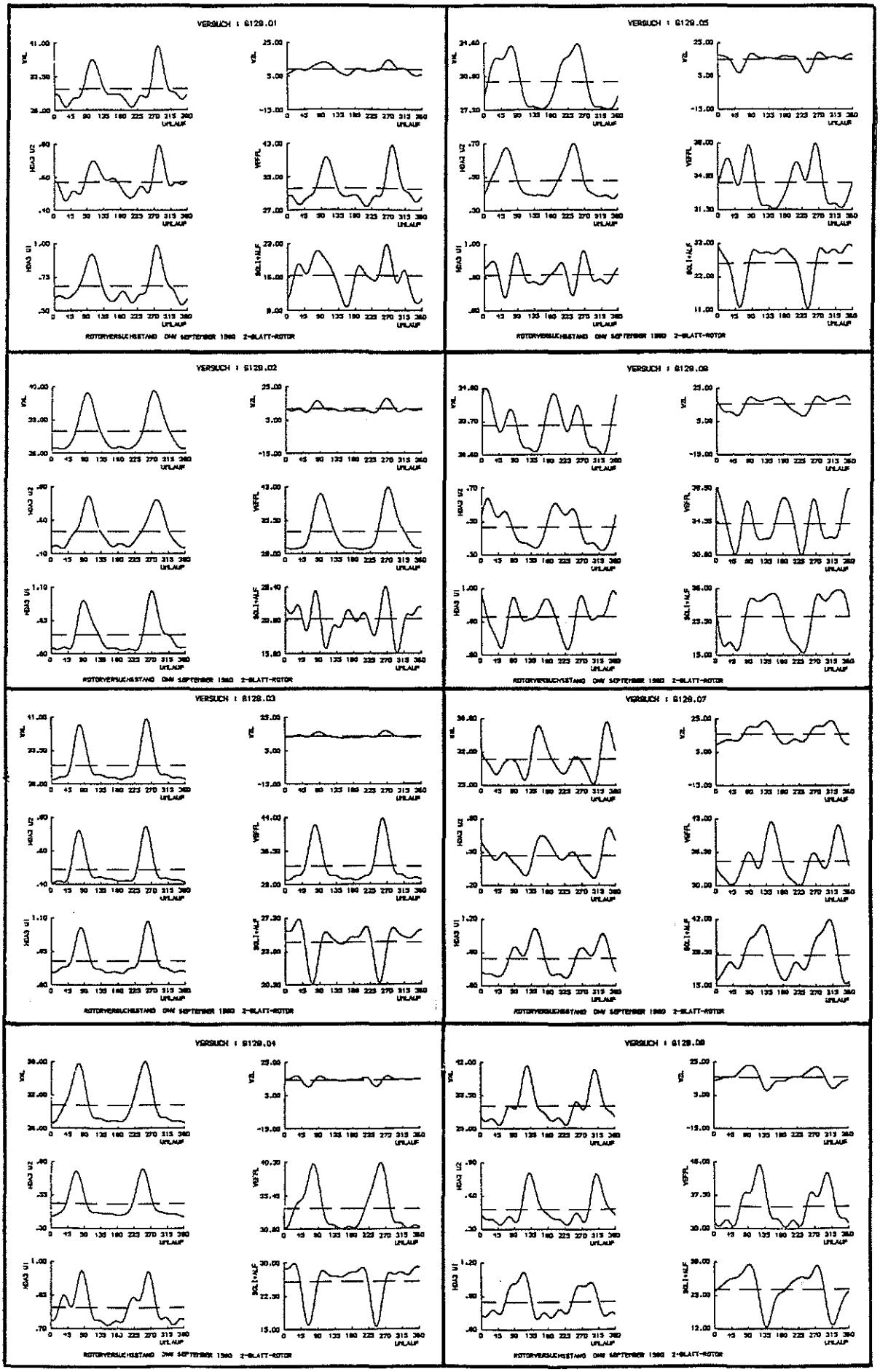

Fig. 6 Computer plotted hot-wire signals

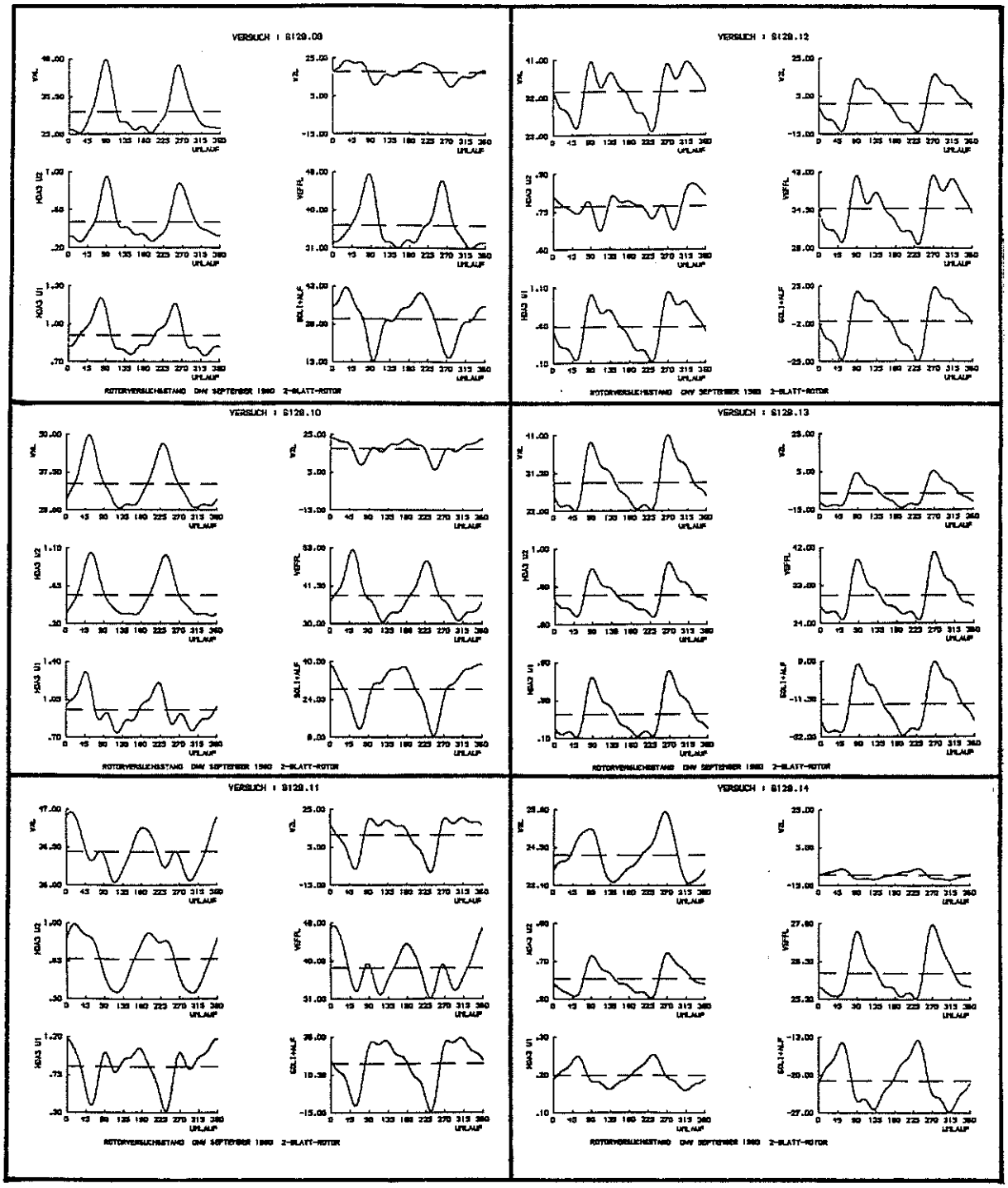

Fig. 6: Continued

Definition:

HDA3 U1
HDA3 U2 } Voltage signals of the X-probe

WXL
WZL } Calibrated velocity components (m/sec)

VEFFL : Magnitude of velocity (m/sec)

SOLI+ALF : Angle of flow-incidence, referred to body fixed axis in the X-Z-plane

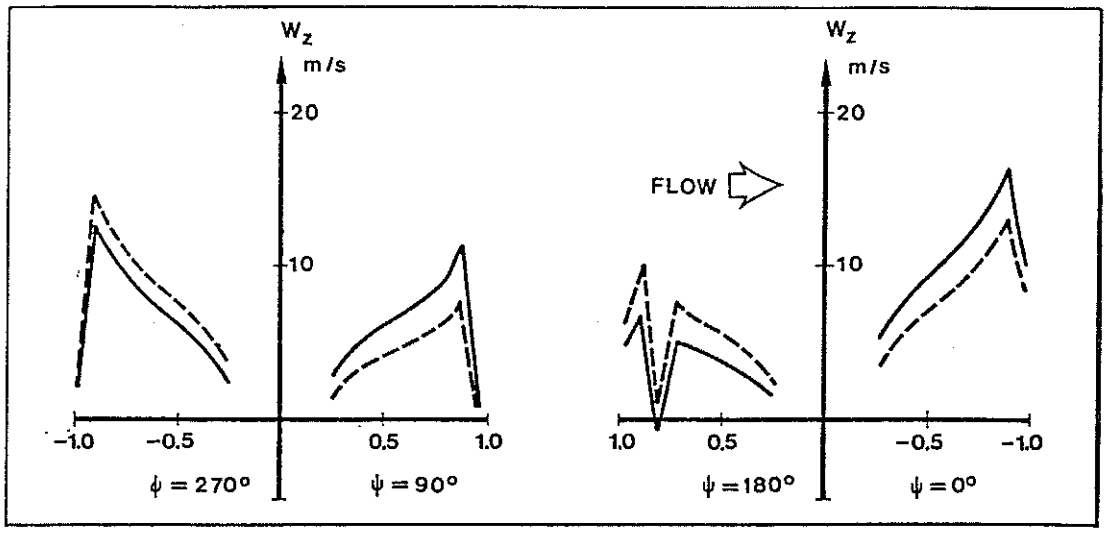

Fig. 7 Local Momentum Theory ($\mu = 0.1$)

— — — without flapping

——— with flapping ($A_1 = -1.55°$, $B_1 = -2.37°$)

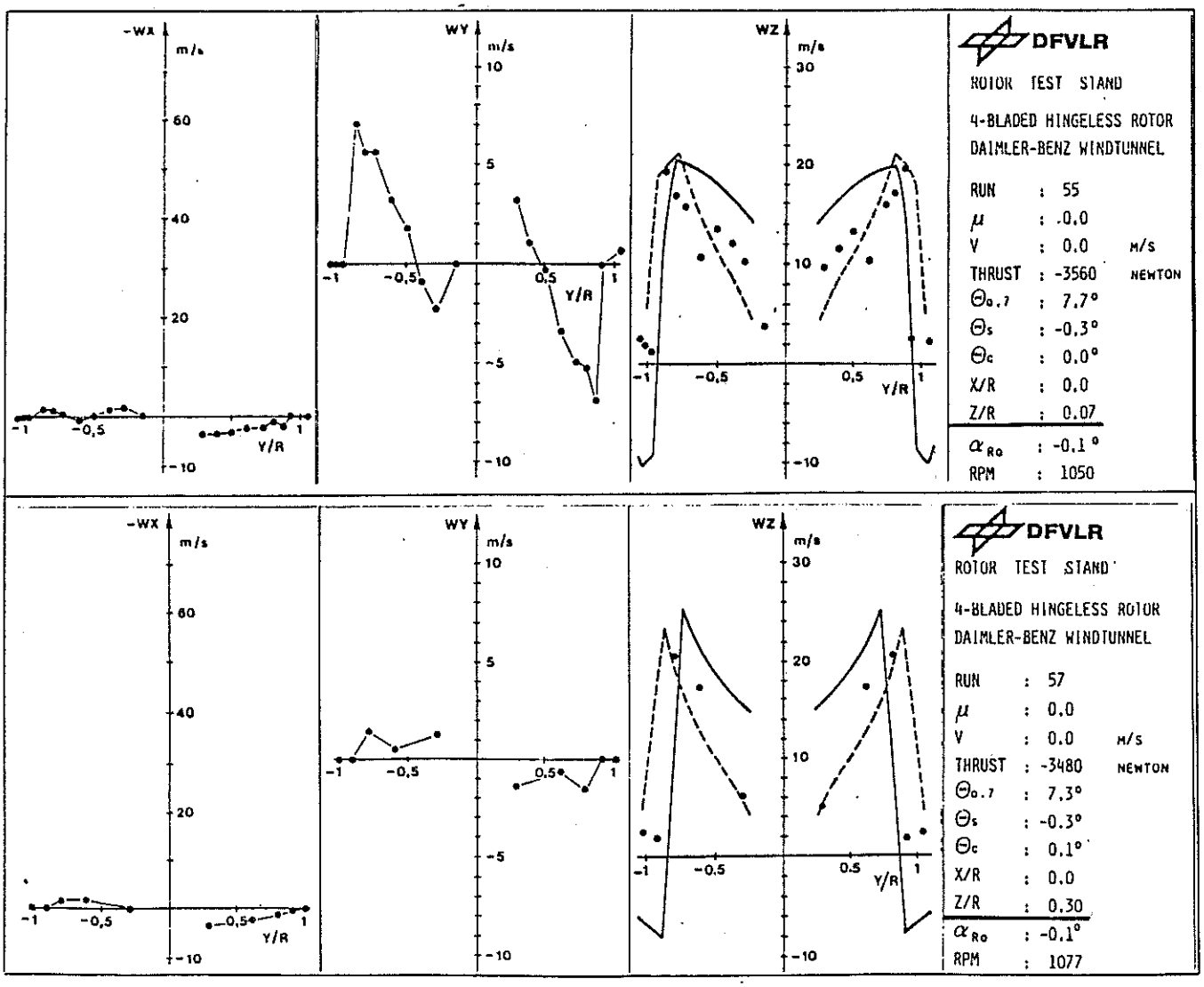

Fig. 8 Comparison of measured and calculated data

• • • Experiment

– – – Theory, Local Momentum

——— Theory, Rigid Vortex

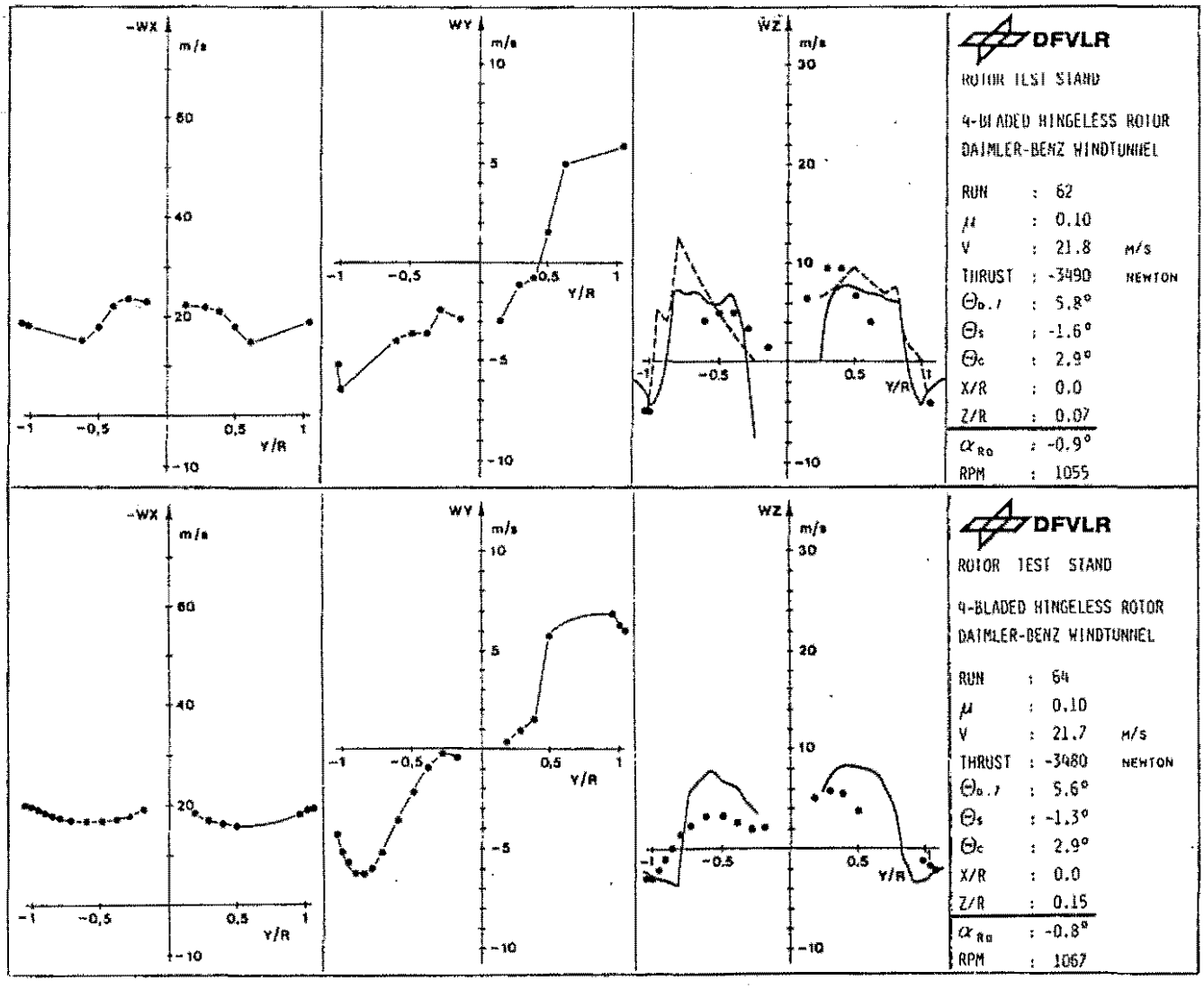

Fig. 9 Comparison of measured and calculated data

• • • Experiment

– – – Theory, Local Momentum

——— Theory, Rigid Vortex

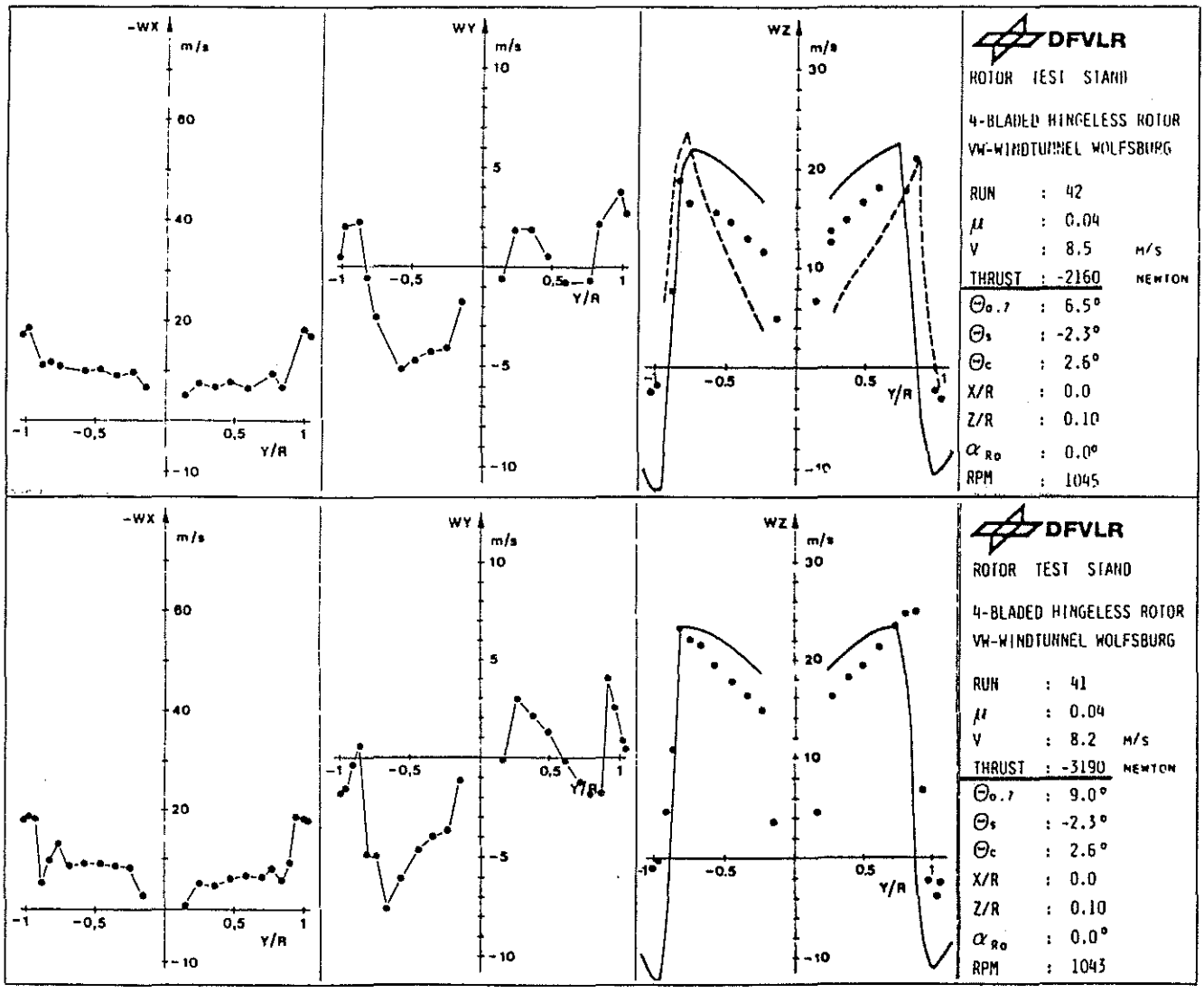

Fig. 10 Comparison of measured and calculated data

● ● ● Experiment

– – – Theory, Local Momentum

——— Theory, Rigid Vortex

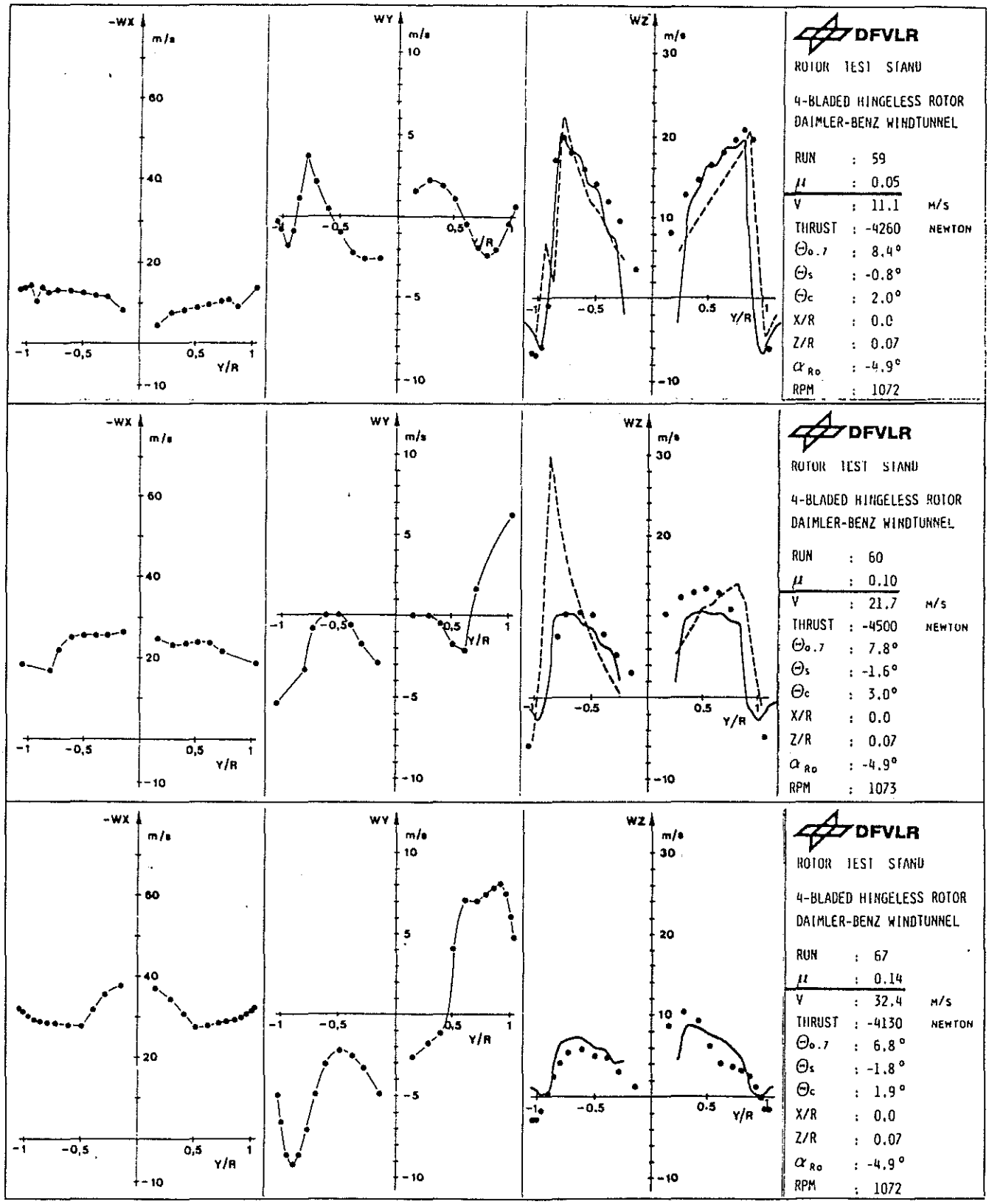

Fig. 11 Comparison of measured and calculated data

• • • Experiment

– – – Theory, Local Momentum

——— Theory, Rigid Vortex

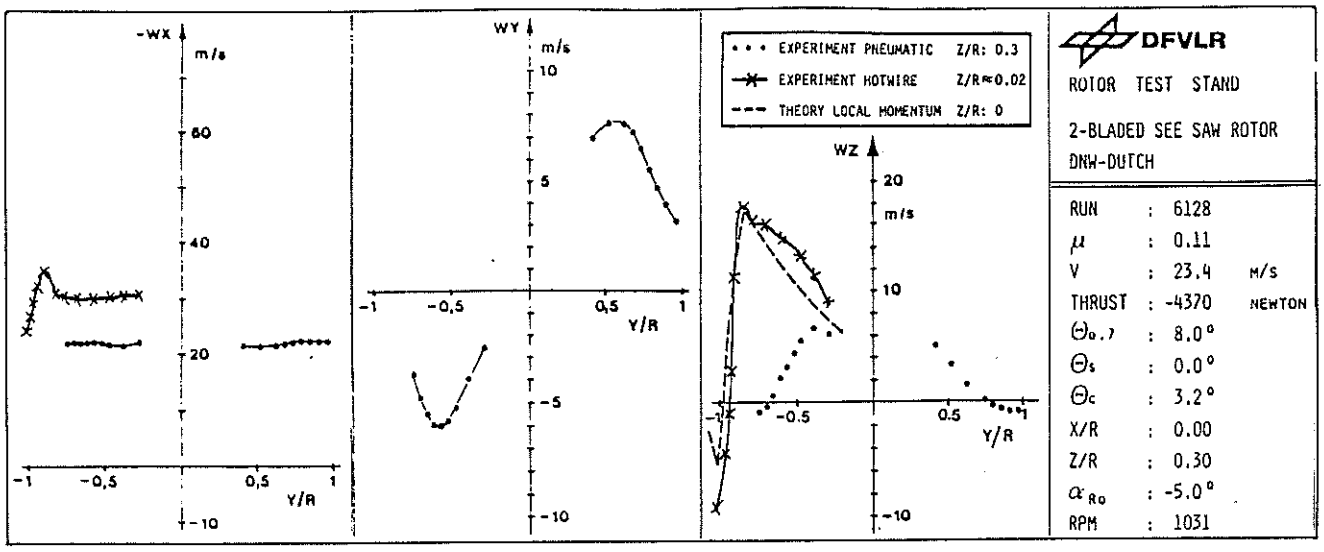

Fig. 12 Comparison of measured and calculated data (2-bladed rotor)

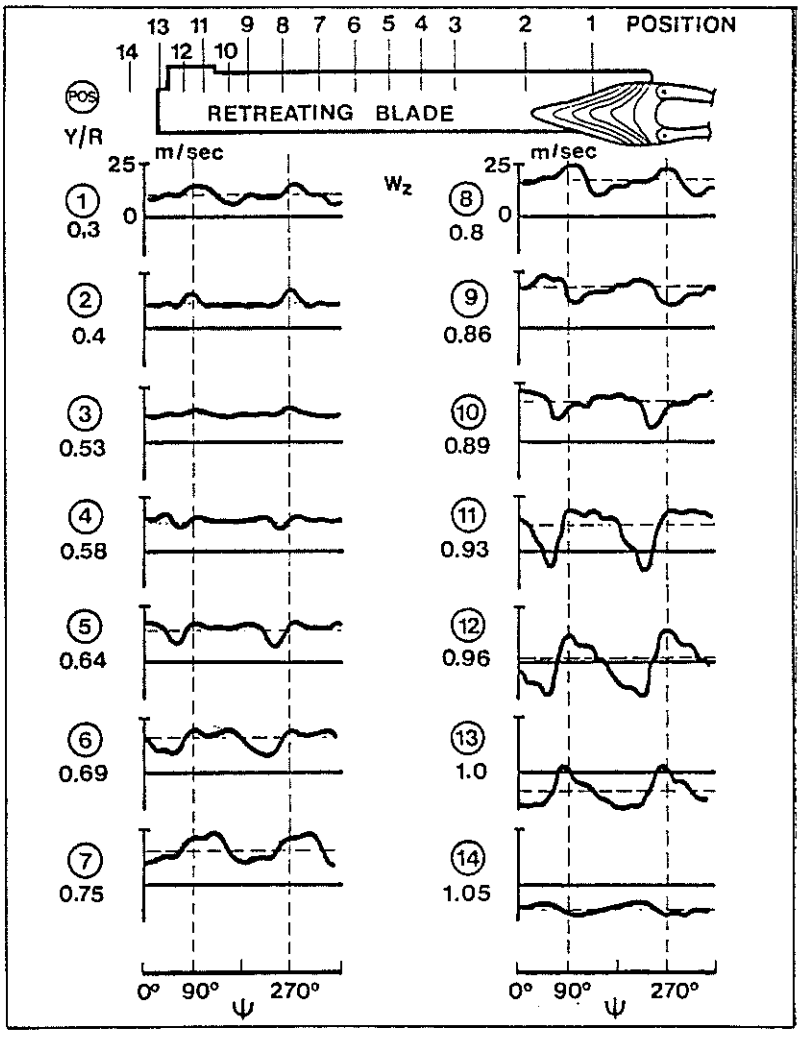

Fig. 13 Time history of unsteady rotor induced velocities measured by a X-probe hot-wire anemometer